Journal of Rock Mechanics and Geotechnical Engineering 18 (2026) 4094–4107

Contents lists available at ScienceDirect

Journal of Rock Mechanics and Geotechnical Engineering

journal homepage: www.jrmge.cn

Full Length Article

Advancing drilling parameter reliability: A data-driven comparison of MWD and DPM for stratigraphic identification

Ping-Feng Li [a,b,c], Xue-Fan Wang [a,b,*], Zhou Yang [b], Zhong-Jian Zhang [b], Fei Yang [c,d], Hong-Pei Tang [c,d], Bing-Bing Zhang [c,d]

[a] Key Laboratory of Safety Intelligent Mining in Non-coal Open-pit Mines, National Mine Safety Administration, Guangdong, Guangzhou, 510000, China
[b] Department of Civil Engineering, China University of Geosciences (Beijing), Beijing, 100000, China
[c] Hongda Blasting Engineering Group Co., Ltd., Guangdong, Guangzhou, 510000, China
[d] School of Mines, China University of Mining and Technology, Jiangsu, Xuzhou, 221000, China

ARTICLE INFO

Article history:
Received 10 April 2025
Received in revised form
20 May 2025
Accepted 29 June 2025
Available online 4 July 2025

Keywords:
Measurement while drilling
Drilling process monitoring
Ground investigation
Drilling speed

ABSTRACT

Stratigraphic interface characterization and strength parameter assessment of geomaterials constitute fundamental research priorities in geological and geotechnical engineering. While measurement while drilling (MWD) and drilling process monitoring (DPM) have emerged as critical techniques for acquiring real-time drilling parameters, inherent limitations in data interpretation persist. The critical challenge of random fluctuations in MWD-derived penetration rate measurements exhibits poor correlation with the stratified homogeneity characteristics of geological formations. Such discrepancies undermine the reliability of stratigraphic classification and mechanical property analysis. Through systematic comparison of MWD and DPM datasets combined with quantitative parameter evaluation, this investigation reveals significant methodological distinctions in data acquisition accuracy. Machine learning-enhanced analysis employing Support Vector Machine (SVM) algorithms demonstrates that DPM-derived parameters provide superior stratigraphic identification capabilities. Our findings indicate that DPM implementations achieve 20.57 % and 38.01 % higher resolution in interface detection along two drillholes compared to the conventional MWD approaches. This improvement allows for better prediction of stratigraphic profiles and more precise guidance in subsequent geological and geotechnical engineering practices.

© 2026 Institute of Rock and Soil Mechanics, Chinese Academy of Sciences. Published by Elsevier B.V. This is an open access article under the CC BY-NC-ND license (http://creativecommons.org/licenses/by-nc-nd/4.0/).

1. Introduction

In geological and geotechnical engineering, acquiring accurate stratigraphic information is essential. Traditional geological drilling methods involve direct sampling of geotechnical lithologies, which are then analyzed through on-site descriptions and laboratory tests to determine their physical and mechanical properties. While effective, these methods are often costly, time-consuming, and may not meet the timeliness requirements of engineering projects (He et al., 2024; Jamshidi et al., 2024; Liu et al., 2024a; Xie et al., 2024; Pirhadi et al., 2025). Additionally, in complex geological environments, such as those with structural planes or weak zones, discontinuities in core samples can lead to incomplete data, compromising both the accuracy and integrity of the findings (Jalili et al., 2020; Wang et al., 2023a; Deng et al., 2024; Liu et al., 2024b).

With the technological advancement of electronic sensors and data acquisition systems, application of the measurement while drilling (MWD) in geological and geotechnical engineering is becoming increasingly widespread. MWD method collects drilling parameters in depth series, including rotation speed, torque, thrust, and penetration rate (Kianoush et al., 2022; Tian et al., 2024; Zhao et al., 2024). These parameters effectively characterize the physicomechanical properties of rock lithologies and are widely used in stratigraphic classification, stratigraphic interface identification, and weak layer detection (Handhal et al., 2022; Xu et al., 2022; Bahrami et al., 2024; Long et al., 2024; Song et al.,

* Corresponding author. Key Laboratory of Safety Intelligent Mining in Non-coal Open-pit Mines, National Mine Safety Administration, Guangdong, Guangzhou, 510000, China.
E-mail address: wangxuefan@cugb.edu.cn (X.-F. Wang).

Peer review under responsibility of Institute of Rock and Soil Mechanics, Chinese Academy of Sciences.

https://doi.org/10.1016/j.jrmge.2025.06.005
1674-7755/© 2026 Institute of Rock and Soil Mechanics, Chinese Academy of Sciences. Published by Elsevier B.V. This is an open access article under the CC BY-NC-ND license (http://creativecommons.org/licenses/by-nc-nd/4.0/).

2025). However, despite its potential in geotechnical engineering, the random variation in penetration rate with depth does not align with the blocky homogeneous nature of underground geotechnical lithologies (Schunnesson, 1998; Gui, 2008; Li et al., 2014; Rai et al., 2015; Mohammadrezaei et al., 2020; van-Eldert et al., 2020).

Drilling process monitoring (DPM) analysis method represents an advancement over MWD method (Yue et al., 2002, 2004; Yue, 2014; Wu et al., 2023), effectively addressing the limitations of MWD method. By employing real-time series analysis, DPM method refines the drilling process by excluding auxiliary operation time and recalculating the drilling speed (Wang et al., 2023b, 2023d). This newly derived drilling speed aligns with the homogeneous distribution characteristics of subsurface geomaterials, thereby offering more reliable data for assessing geomaterials conditions (Mostofi et al., 2011; Alipour, 2024). The zoning results and strength classifications generated by DPM method show strong correlation with the structural interfaces and strength properties observed in core samples (Pireh et al., 2015; Wang et al., 2023c, 2023d).

Table 1 provides a summary of relevant studies comparing MWD and DPM methods in geological and geotechnical engineering. MWD method recorded drilling information only corresponding to the drill bit advancement at a pre-assigned depth advancement increment, such as 5 mm, 10 mm, 50 mm, and 100 mm. DPM method acquired drilling parameters in real-time series, usually at a frequency of 1 s.

This paper compares the drilling parameters of MWD and DPM methods using real-time data, providing a quantitative analysis to illustrate accuracy differences. The evaluation focuses on drilling speed, which is crucial for stratigraphic interface classification and strength assessment. Additionally, variations in downward pressure, upward pressure, and rotation speed for each method are analyzed. Parameters from both methods are utilized for stratigraphic interface classification. This comparison highlights the accuracy and benefits of DPM method in assessing rock structural interfaces and determining the physicomechanical properties of rocks.

2. Difference between MWD and DPM methods

2.1. Comparison of MWD and DPM algorithm

2.1.1. Different calculation of MWD penetration rate and DPM drilling speed

Drilling speed refers to as the depth the drill bit penetrates the formation per unit of time, typically measured in m/h or ft/h. It serves as a crucial indicator of drilling efficiency, influenced by factors such as drill bit type, formation characteristics, drilling fluid properties, and drilling rig power. Enhancing drilling speed can significantly shorten the drilling cycle and reduce costs, making its optimization a key technical and economic objective along drilling operations. In MWD method, this is referred to as the penetration rate, whereas in DPM method, it is described as drilling speed (Wu et al., 2024; Yue et al., 2024).

In order to understand the effects of MWD and DPM analysis methods in geotechnical engineering, this section will compare and analyze the average MWD penetration rate and DPM drilling speed of drillholes A and B at different depth intervals. The random variation of MWD penetration rate is mainly caused by the pre-assigned depth increment method (Wang et al., 2023b). This method is widely used to record the drilling parameters of MWD system. The pre-assigned depth interval sampling method selects the pre-assigned depth interval $\Delta H_{j,\mathrm{pre-assigned}}$, and measure the measurement time for each depth interval $\Delta t_{j,\mathrm{measured}}$. Then we can get the average penetration rate of a depth interval, calculated by (Wang et al., 2021):

$$H_i = \frac{\Delta H_{j,\mathrm{pre-assigned}}}{\Delta t_{j,\mathrm{measured}}} \tag{1}$$

where H_i is the average penetration rate at depth.

Then, the factual drilling data set can be rearranged by adding a new time sequence of one regular time increment by (Wang et al., 2024):

Table 1
Literature on drilling parameters.

MWD method		
Depth series (mm)	Case study	Source
5	Detection of ground strata using instrumented borehole drilling in Kennington Park reveals new interpretation methods despite limited correlation with undrained strength data	Gui et al. (2002)
	Detection of soil properties using digital drilling parameters recorders enhances monitoring and reduces study costs	Pfister (1985)
10	Determine the soil profile of the Saline di Augusta site	Garassino and Schinelli (1998)
	Detection of cavities by monitored borehole drilling	Fortunati and Pelligrino (1998)
50	Application of monitored borehole data for material identification is explored through three case studies	Peck and Vynne (1993)
100	Detection of ore boundaries and fractures by stepwise normalization of monitored drilling data in Swedish crystalline rock	Schunnesson (1998)
DPM method		
Real-time series (s)	Case study	Source
1	Use of HKU drilling process monitor in slope stabilization	Yue et al. (2002)
	Detection of volcanic weathering zones using in situ digital monitoring in rotary-percussion drilling offers a cost-effective geotechnical investigation method	Yue et al. (2004)
	In situ strength profiles along two adjacent vertical drillholes from digitalization of hydraulic rotary drilling	Wang et al. (2023b)
	Detection of rock weathering grades through in-situ drilling monitoring shows strong potential for ground characterization	Chen and Yue (2015)
	Detection of soil and rock strength profiles using digital DPM along a 200 m drillhole in Xi'an enhances in-situ exploration capabilities	Wang et al. (2021)
	Detection of ground conditions for the Wu-Kai Expressway tunnel enhances weathered argillaceous limestone profiling using advanced drilling and MWD data analysis	Wu et al. (2024)

$$n = \sum_{j=0}^{k-1} \left(T_{jM_j} - T_{j0}\right) + (T_{km} - T_{k0}) \tag{2}$$

where n is the n-th net drilling time, and $n = 0, 1, 2, \ldots, N$, where N represents the last net drilling time along each drillhole, $N = \sum_{k=1}^{K} M_k$; and T_{jM_j} represents the M_j-th sampling time along the j vertical advancement of chuck, where M_j represents the last sampling time along the j vertical advancement of chuck.

Given the high rigidity and stiffness of the connected extension rods and drill bit, there is negligible elongation or shortening during net drilling time. Therefore, the drilling depth during net drilling time is calculated by (Wang et al., 2024):

$$Depth_{DPM}(n) = \sum_{j=0}^{k-1} DPM_{\text{advancement}}\left(T_{jM_j}\right) + DPM_{\text{advancement}}(T_{km}) \tag{3}$$

where $Depth_{DPM}(n)$ represents the accumulated drilling depth at the n-th net drilling time, $Depth_{DPM}(0)$ represents the starting depth, and the starting depths along three drillholes in this case are all 0.000 m; and $DPM_{\text{advancement}}\left(T_{jM_j}\right)$ represents the vertical advancement during the sampling time period of T_{j0} to T_{jM_j}.

The drilling process can be divided into different linear segments according to different drilling speeds. In the net drilling process, the determination of the constant drilling speed in each linear region can be calculated by (Wang et al., 2024):

$$D_{si} = \frac{DPM_{\text{displacement}}(t_i + \Delta t_i) - DPM_{\text{displacement}}(t_i)}{\Delta t_i} \tag{4}$$

where D_{si} is the constant drilling speed of the i-th linear zone during net drilling process, which is equal to the slope gradient of the linear segment; $DPM_{\text{displacement}}$ is the monitored factual data of chuck displacement; t_i is the starting time of the i-th linear zone during the net drilling process ($i = 1, 2, 3, \ldots, n$, n is the last linear zone of net drilling process along the drillhole); and Δt_i is the elapsed time of the i th linear zone during the net drilling process.

2.1.2. Comparison of MWD and DPM original field data from drillholes A and B

In field, the monitoring framework comprises three integrated components: displacement, pressure, and rotation. These subsystems autonomously capture digitized factual measurements through electrical signaling in real-time temporal sequences, corresponding to drill bit progression, vertical displacement hydraulic forces, and rotational velocity. The measurement precision of respective transducers reaches 0.001 m for positional accuracy, 0.001 MPa for pressure resolution, and 1 r/s for rotational frequency detection. The configuration enables concurrent acquisition of four distinct voltage-based signals through synchronous sampling at 1-s interval. For experimental validation, two adjacent vertical drillholes were excavated using one hydraulically-driven rotary drilling machine with one polycrystalline diamond drill bit. The monitoring system can automatically record digital data as electrical signals in real-time series. This system is portable, easy to install, and causes minimal interference with either the drilling equipment or routine on-site operations during the drilling process.

According to Eqs. (1)–(4), both MWD penetration rate and DPM drilling speed were calculated by the original field drilling data along two drillholes. The coefficient of variation (CV) was used to quantify the random variation in the penetration rate of MWD method and the drilling speed of DPM method. The CV, a key statistical measure, reflects data dispersion and is defined as the ratio of the standard deviation (SD) to the mean (Shechtman, 2013). A higher CV indicates greater random variation in the data. To evaluate the differences between MWD and DPM methods, the percentage difference along drilling speed between the two was calculated. The percentage difference is determined as follows:

$$Differences\% = \frac{P_{\text{DPM}} - P_{\text{MWD}}}{P_{\text{DPM}}} \times 100\% \tag{5}$$

where P_{DPM} is the drilling parameter after DPM analysis, and P_{MWD} is the drilling parameter after MWD method.

The original data consist of real-time series data collected by DPM system with a sampling interval of 1 s. This section analyzes the data using both DPM and MWD methods. MWD method evaluates the data at pre-assigned depths of 1 m, 0.5 m, 0.2 m, 0.1 m, and 0.05 m. To compare the methods, this section focuses on two specific depth intervals. It compares the average penetration rate of MWD method at pre-assigned depths of 0.5 m and 0.1 m with the drilling speed obtained by DPM method through the depth-time curve.

Fig. 1 shows the comparison of MWD penetration and DPM drilling speed from 32.40 to 33.50 m along drillhole A. Fig. 1a shows MWD penetration rate variation curve with depth at a pre-assigned depth of 0.05 m. The average MWD penetration rate in this area is 0.300 m/min, and $CV = 32.9$ %. This CV value shows that the average penetration rate of MWD method at this pre-assigned depth has a certain random variability, but it remains relatively stable overall. Fig. 1b shows the average MWD penetration rate variation curve with depth at a pre-assigned depth of 0.1 m. The average MWD penetration rate in this area is 0.351 m/min, and $CV = 29.1$ %. Fig. 1c shows the net drilling time variation curve with depth. In this area, DPM drilling speed is 0.336 m/min, and the linear correlation coefficient is 0.99602. Similarly, the penetration rate at both pre-assigned depths of MWD method shows some random variability, but the level of random variation is relatively low, and the average speed is quite different, with a difference rate of 17 %. The area is divided into 15 linear regions by DPM method. Within the linear range, DPM drilling speed is constant. Therefore, the drilling speed will change with the change of rock strength, not randomly.

Fig. 2 shows comparison of MWD penetration rate and DPM drilling speed from 0.00 m to 1.55 m along drillhole B. Fig. 2a shows the average MWD penetration rate curve with depth at a pre-assigned depth of 0.05 m. The average MWD penetration rate in this area is 2.428 m/min, and $CV = 128.6$ %. Fig. 2b shows the average MWD penetration curve with depth at a pre-assigned depth of 0.1 m. The average MWD penetration rate in this area is 1.477 m/min, and $CV = 125.9$ %. Fig. 2c shows the net drilling time curve with depth. In this area, DPM drilling speed is 2.218 m/min, and the linear correlation coefficient is 0.9945. Similarly, the average MWD penetration at both pre-assigned depths shows partial random variability, and the level of random variation is extremely high, and the average penetration rate is quite different, with a difference rate of 17 %. This section of DPM is divided into linear sub-area No. 1, and the drilling speed will change with the change of rock strength, not randomly.

2.1.3. Comparison of MWD penetration rate and DPM drilling speeds from drillholes A and B

In this section, two different depth intervals are selected to compare the average drilling speed of MWD method at pre-assigned depths of 0.0.5 m and 0.1 m with DPM drilling speed in these depth intervals.

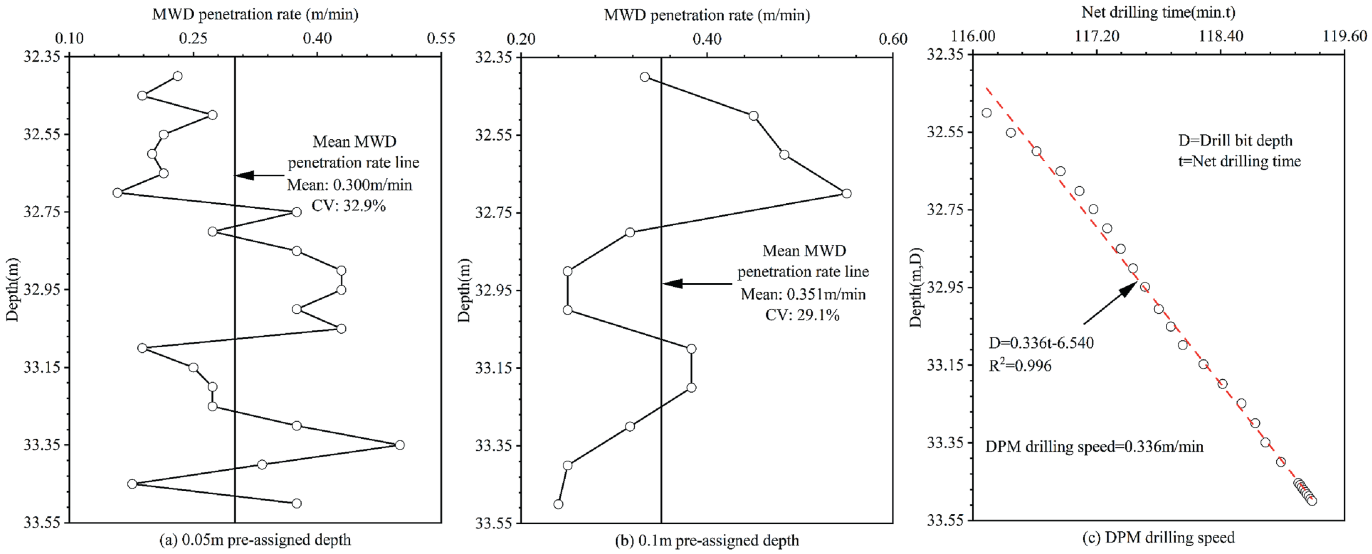

Fig. 1. Comparison of MWD penetration rate and DPM drilling speed from 32.40 m to 33.50 m along drillhole A: (a) 0.05 m pre-assigned depth, (b) 0.1 m pre-assigned depth, and (c) DPM drilling.

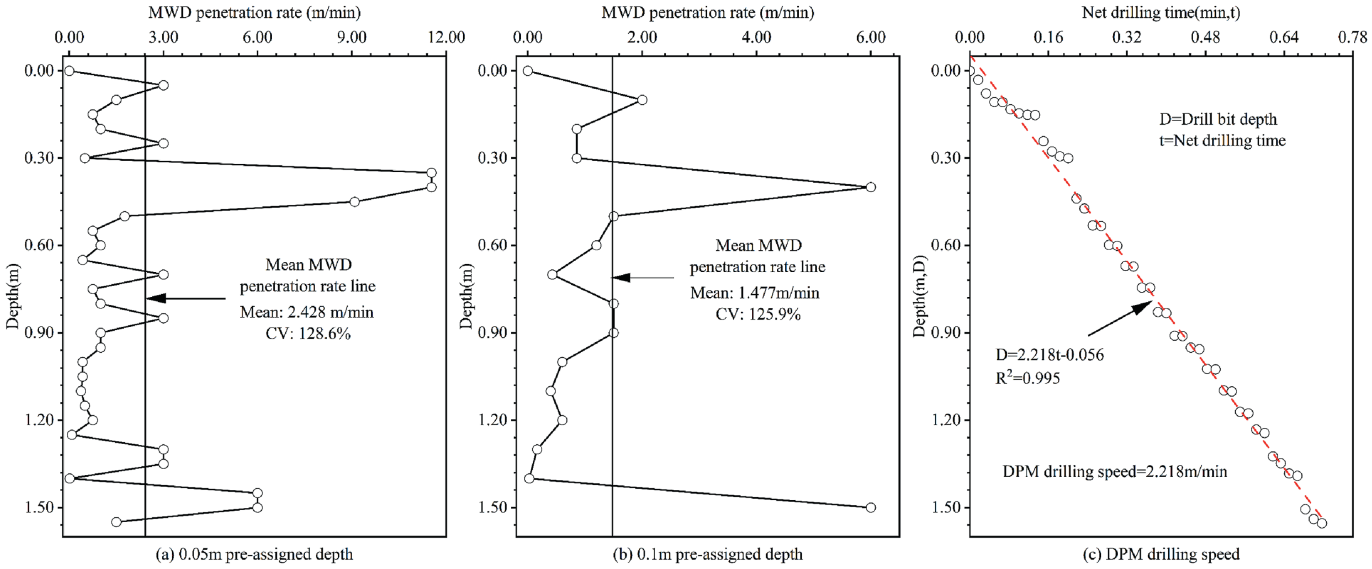

Fig. 2. Comparison of MWD penetration rate and DPM drilling speed from 0.00 m to 1.55 m along drillhole B: (a) 0.05 m pre-assigned depth, (b) 0.1 m pre-assigned depth, and (c) DPM drilling speed.

Fig. 3 illustrates a comparison of the average MWD penetration rate and DPM drilling speed at various pre-assigned depths ranging from 32.0 m to 33.7 m along drillhole A. Fig. 3a shows the average MWD penetration rate curve with depth at a pre-assigned depth of 0.05 m. The average MWD penetration rate in this area is 1.817 m/min, and the CV = 54.5 %. Fig. 3b shows MWD method with a pre-assigned depth of 0.1 m. In this case, the average MWD penetration rate in this area is 1.545 m/min, and CV = 57.6 %. Fig. 3c indicates that each sub-area corresponds to a constant drilling speed, with a total of 31 sub-areas identified; the drilling speed varies according to the geomaterial strength.

Fig. 4 compares the average MWD penetration rate with DPM drilling speeds at different pre-assigned depths from 13.00 m to 18.00 m along drillhole B. Specifically, Fig. 4a shows the variation curve of the average MWD penetration rate with depth when the pre-assigned depth is 0.05 m. The average drilling speed measured by MWD method is 0.057 m/min, and CV = 54.4 %. Fig. 4b shows the change curve of the average MWD penetration rate with depth when the pre-assigned depth is 0.1 m. The average MWD penetration rate is 0.053 m/min, and CV = 55.9 %. Fig. 4c shows the drilling speed of DPM in this area. The area is divided into 54 linear segments, and the drilling speed changes with the change of geomaterial strength.

Comparative analysis indicates that, regardless of whether the pre-assigned depth is 0.05 m or 0.1 m, MWD method's average penetration rate shows significant random variation across different depth intervals in the two drillholes. This variability is inherent to MWD method, where the penetration rate is calculated as the ratio of the pre-assigned advancement depth interval to the total time taken for that section. This represents an instantaneous measurement, making it prone to fluctuations from minor changes in either the depth interval or the total time. In contrast, DPM method

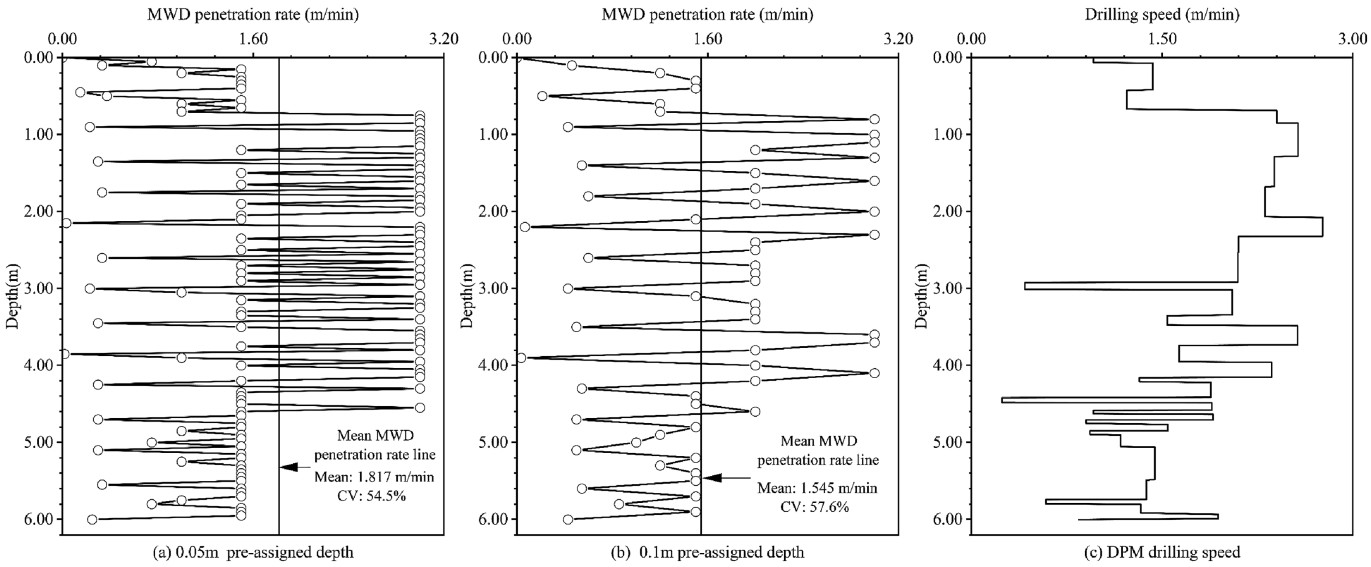

Fig. 3. Comparison of the average MWD penetration rate and DPM drilling speeds at different pre-assigned depths from 0.00 m to 6.00 m along drillhole A: (a) 0.05 m pre-assigned depth, (b) 0.1 m pre-assigned depth, and (c) DPM drilling speed.

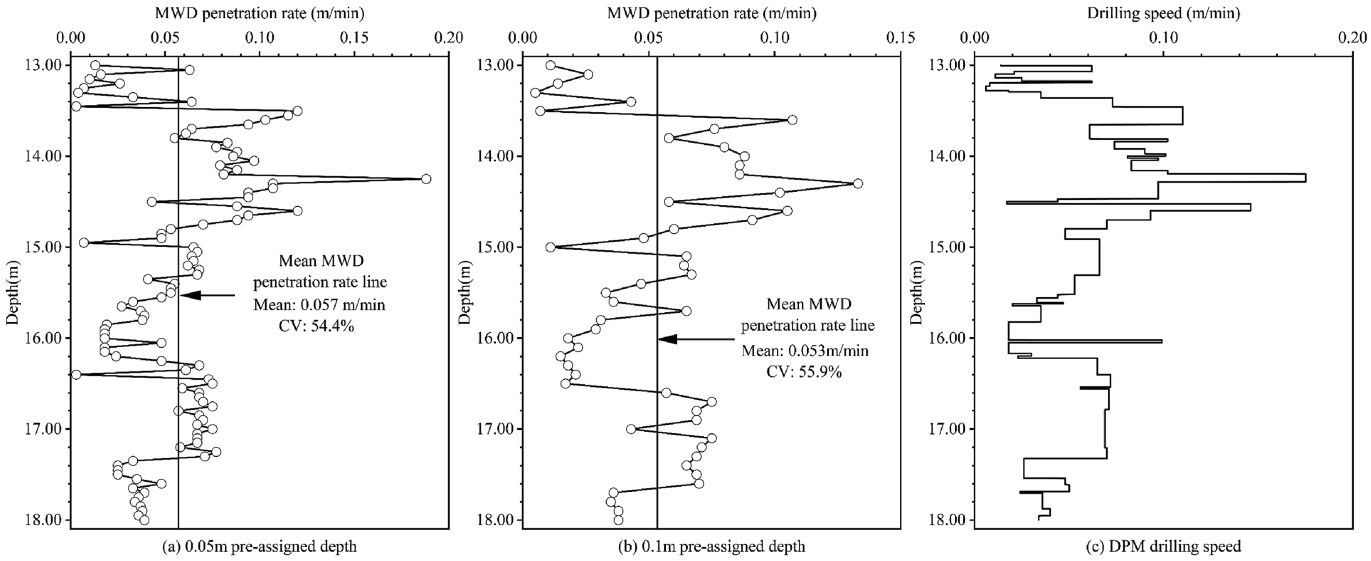

Fig. 4. Comparison of the average MWD penetration rate and DPM drilling speeds at different pre-assigned depths from 13.00 m to 18.00 m along drillhole B: (a) 0.05 m pre-assigned depth, (b) 0.1 m pre-assigned depth, and (c) DPM drilling speed.

determines drilling speed by calculating the slope of the curve that represents the relationship between drill bit advancement depth and net drilling time. As an integral approach, it effectively reduces the impact of minor variations in depth advancement and drilling time on velocity measurements. Consequently, DPM method significantly minimizes the high random variation observed in MWD method.

The considerable random variation in MWD method primarily stems from the random vibrations of the drilling rig during operation, which significantly impacts the average penetration rate. Penetration rate serves as a crucial indicator for assessing stratigraphic interface characteristics, playing a vital role in the ground characterization and engineering geological evaluation of drilling methods (Chen et al., 2022; Li et al., 2017). Therefore, accurate drilling speed parameters are essential for understanding underground structures and conducting reliable engineering geological assessments.

2.2. Comparative analysis of key parameters of the drilling process

In geological exploration and engineering design, accurately assessing the physical properties of stratigraphic interface is essential (Wang et al., 2019). This requires a thorough analysis of key drilling parameters, including downward pressure, upward pressure, and rotation speed. These parameters not only govern the interaction between the drill bit and the rock but also provide insights into the mechanical behavior of the stratigraphic interface. Downward pressure and rotation speed are particularly critical in influencing drilling efficiency. Downward pressure directly acts on the drill bit, facilitating its penetration into the

rock, while rotation speed impacts the effectiveness of rock fragmentation. By optimizing these two parameters, it is possible to enhance drilling speed and minimize damage to the stratigraphic interface structure, thereby preserving its original state. This optimization yields reliable data for subsequent geological analyses. Upward pressure is closely related to the stratigraphic interface's friction coefficient, the weight of the drill bit, and the depth of the drillhole. By measuring upward pressure, one can evaluate the friction and resistance encountered by the drill bit, leading to a better understanding of the stratigraphic interface's physical characteristics. This evaluation is vital for predicting potential challenges during drilling and developing appropriate response strategies.

Fig. 5 illustrates the variations along drilling parameters with depth along drillhole A, comparing results from MWD method (with a pre-assigned depth increment of 0.05 m) and DPM method. Specifically, Fig. 5a highlights the changes in downward pressure as a function of depth for both methods. The findings reveal that downward pressure remains nearly identical across the depth range for both MWD and DPM, exhibiting only minor random fluctuations at certain points. The CV for downward pressure is 8.3 % for MWD and slightly lower at 7.1 % for DPM. Despite these slight differences, DPM method demonstrates greater consistency and precision overall, as evidenced by its lower CV and SD. This supports the conclusion that DPM method provides more accurate and stable results when evaluating drilling parameters. Fig. 5b compares the variations in upward pressure along the depth of the drillhole for both MWD and DPM methods. The results indicate that the upward pressures are largely consistent between MWD and DPM. The CV for MWD upward pressure is 35.3 %, while for DPM, it is lower at 26.2 %. Notably, compared to downward pressure, the upward pressure shows greater variability between MWD and DPM. Fig. 5c presents a comparison of rotation speed along the depth of the drillhole. The CV for MWD rotation speed along drillhole A is 9.1 %, whereas the CV for DPM rotation speed is slightly lower at 8.1 %.

Fig. 6 provides a detailed comparison of the changes in downward pressure, rotation speed, and upward pressure with depth along drillhole B, utilizing both MWD and DPM methods (with a pre-assigned depth increment of 0.05 m). Fig. 6a focuses on the variations in downward pressure between MWD and DPM. Along drillhole B, the CV for downward pressure measured by MWD method is 5.1 %, while that for DPM method is slightly lower at 2.2 %. This indicates similar variability in downward pressure between MWD and DPM. Fig. 6b compares upward pressure changes between MWD and DPM methods. The CV for upward pressure using MWD method is 34.6 %, compared to 22.1 % for DPM method, indicating that DPM method offers greater stability. Fig. 6c illustrates the changes in rotation speed for both methods. Along drillhole A, the rotation speed CV for MWD method is 8.2 %, whereas DPM method shows a lower coefficient of 3.8 %, indicating superior stability in rotation speed measurement with DPM method.

Compared to drillhole A, drillhole B shows greater SD and CV differences in the measurements of downward thrust, upward pressure, and rotation speed between MWD and DPM methods. However, a detailed analysis of data from both drillholes indicates that these differences are not statistically significant. This suggests that both methods are effective for measuring downward thrust, upward pressure, and rotation speed (see Table 2).

2.3. Influence of drilling parameters on drilling speed

By comparing MWD and DPM drilling parameters, it can be found that the downward pressure, upward pressure, and rotation speed obtained by the two analysis methods are almost the same. Therefore, this chapter further analyzes the changes of these parameters with drilling speed.

Figs. 7 and 8 show the changes of downward pressure, upward pressure, and rotation speed along drillholes A and B with the drilling speed. Fig. 7a indicates that as the constant drilling speed rises from 0.015 m/min to 2.76 m/min, the average downward pressure shows minimal variation. Fig. 7b and c illustrates that as the constant drilling speed increases, the average upward pressure generally trends upward, while the rotation speed trends downward.

Fig. 8 reveals a similar pattern. As the constant drilling speed increases from 0.06 m/min to 2.145 m/min, the average downward pressure, upward pressure, and rotation speed exhibit only minor fluctuations, remaining largely stable. Specifically, Fig. 8a indicates that the average downward pressure does not vary significantly as the constant drilling speed rises from 0.06 m/min to 2.145 m/min.

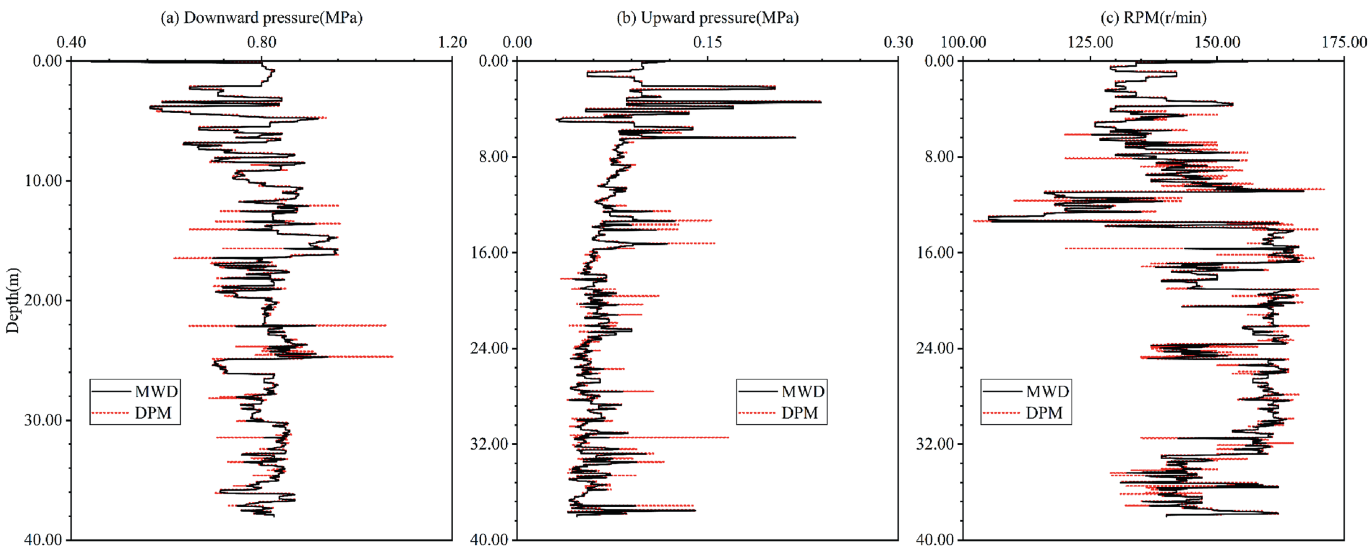

Fig. 5. A comparison of drilling parameters of MWD (pre-assigned depth of 0.05m) and DPM from 0.00 m to 38.07 m along drillhole A: (a) Downward pressure, (b) upward pressure, and (c) rotation speed.

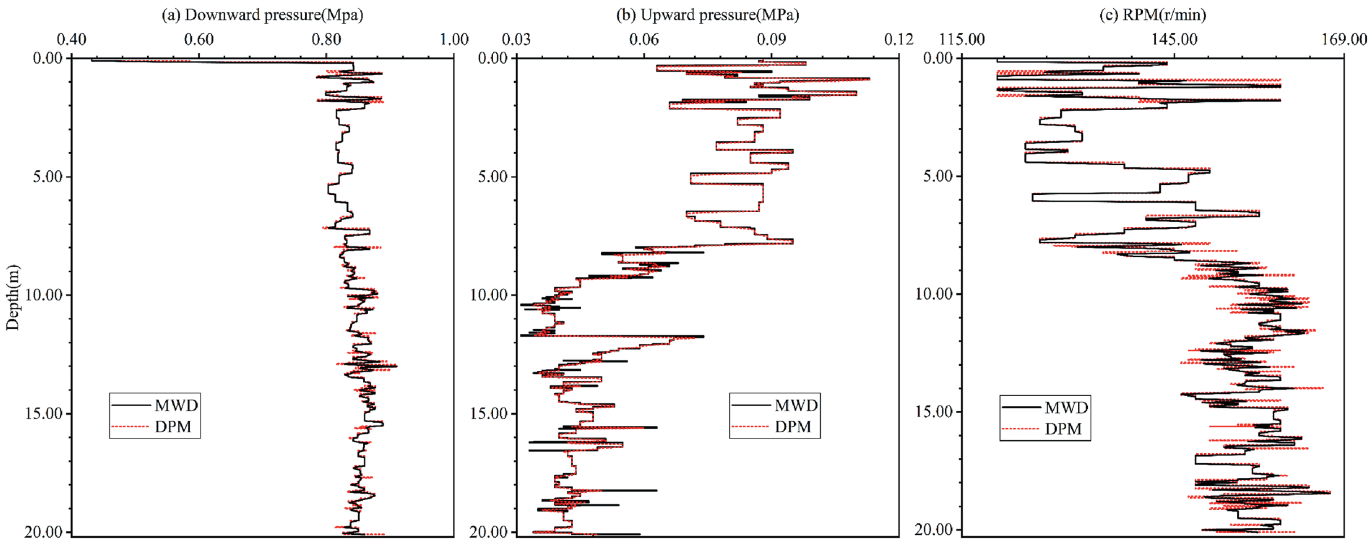

Fig. 6. A comparison of drilling parameters of MWD (pre-assigned depth of 0.05 m) and DPM from 0.00 m to 20.12 m along drillhole B: (a) Downward pressure, (b) Upward pressure, and (c) Rotation speed.

Table 2
Comparison of MWD and DPM drilling parameters along two drillholes.

Drillhole	Analysis method	Downward pressure			Upward pressure			Rotation speed		
		Mean (MPa)	SD (MPa)	CV (%)	Mean (MPa)	SD (MPa)	CV (%)	Mean (r/min)	SD (r/min)	CV (%)
A	MWD	0.804	0.067	8.3	0.070	0.025	35.3	147.546	13.396	9.1
	DPM	0.814	0.058	7.1	0.062	0.016	26.2	149.779	12.153	8.1
B	MWD	0.839	0.043	5.1	0.061	0.021	34.6	147.679	12.169	8.2
	DPM	0.852	0.019	2.2	0.045	0.01	22.1	155.524	5.859	3.8

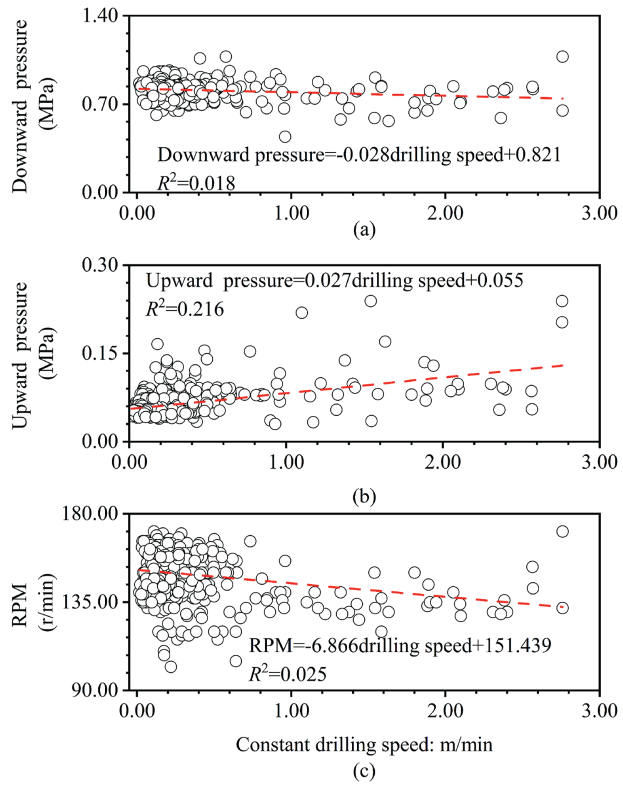

Fig. 7. Influence of drilling parameters on drilling speeds along drillhole A: (a) Downward pressure, (b) Upward pressure, and (c) Rotation speed.

Fig. 8b demonstrates that the average upward pressure remains stable, with a slight downward trend. Fig. 8c confirms that the average rotation speed stays stable, exhibiting an upward trend.

Combining the results from both drillholes on the influence of downward pressure, rotation speed, and upward pressure on drilling speed reveals that as drilling speed increases, these parameters fluctuate within a stable range. This suggests that variations in drilling power parameters do not significantly impact drilling speed. This conclusion aligns with existing literature, which posits that maintaining consistent drilling power parameters allows for an indirect evaluation of the mechanical strength of the stratigraphic interface through drilling speed (Jimeno et al., 1995; Gui et al., 2002; Wu et al., 2023). In this case, the thrust pressure, upward pressure, and rotation are fixed to fluctuate within a certain range of high gear during drilling process. With this method, the analysis results show that the parameters have limited effects on the variations of the drilling speed. The drilling speeds are mainly related to the drilled geomaterial properties along two drillholes. It is an effective method for the collection and analysis of drilling parameters during typical hydraulic rotary drilling. The applicability of this method to different geological environments or under different drilling methods still needs further study.

3. Comparison of drilling parameters between MWD and DPM methods

3.1. Comparison of drilling speeds over the complete drilling process

The previous chapter compared the average MWD penetration rate and DPM drilling speed across various depth intervals,

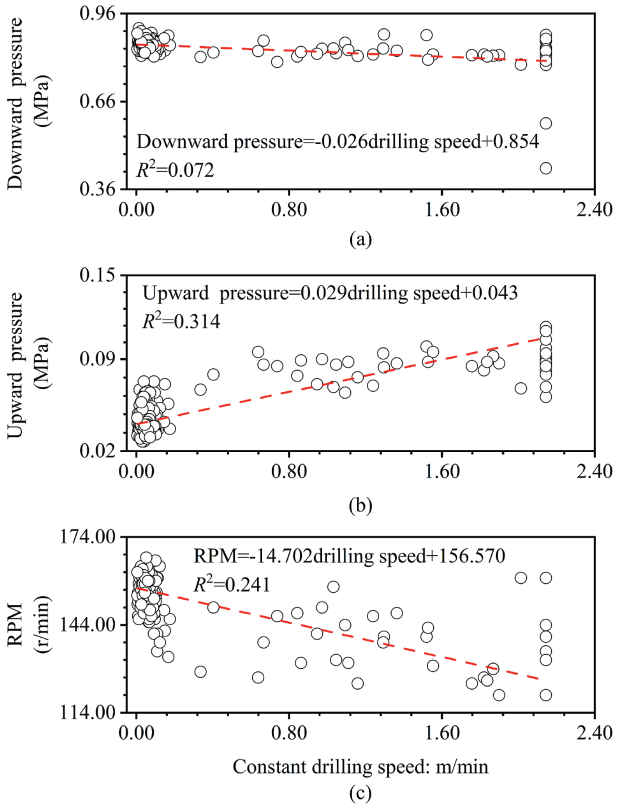

Fig. 8. Influence of drilling parameters on drilling speeds along drillhole B: (a) Downward pressure, (b) Upward pressure, and (c) Rotation speed.

highlighting the random variability of the average MWD penetration rate. This section extends the analysis by comparing MWD at different pre-assigned depths with DPM drilling speeds throughout the entire drilling process. This approach allows for a more intuitive examination of the accuracy differences between MWD and DPM methods during drilling.

Fig. 9 displays the drilling depth and drilling time curves along drillhole A at various pre-assigned depths. Notably, when the pre-assigned depths are set at 1 m, 0.5 m, and 0.2 m, the average drilling speed exhibits significant random variability, with a high level of fluctuation. At a pre-assigned depth of 0.1 m, while the random variability in average drilling speed decreases, it remains notable. This indicates that the average penetration rate of MWD responds to changes in lithological strength; however, the average mechanical penetration speed does not show a direct correlation with lithological strength.

At a pre-assigned depth of 0.05 m, MWD average penetration rate continues to demonstrate random variability, reflecting lithological changes to some extent—the drilling speed tends to decrease as lithological strength increases. The data indicate that the maximum average MWD penetration rate along drillhole A is 3 m/min, which is slightly higher than DPM drilling speed of 2.760 m/min. Additionally, there is a notable difference in the minimum values between MWD and DPM. The distribution of MWD average penetration rate is wider, and its CV value is significantly higher than that of DPM drilling speed. This suggests that MWD average penetration rate is more unstable and exhibits greater variability.

Fig. 10 reveals a similar pattern along drillhole B. At a pre-assigned depth of 1 m, MWD average penetration rate exhibits random fluctuations, with a trend that closely resembles DPM drilling speed; however, there are notable differences between the two. When the pre-assigned depths are set at 0.5 m and 0.2 m, MWD average penetration rate shows a high degree of random variability, diverging significantly from DPM drilling speed and failing to accurately reflect the strength characteristics of the geomaterials.

As the pre-assigned depth decreases to 0.1 m, the average MWD penetration rate approaches DPM drilling speed but still displays considerable randomness. At a depth of 0.05 m, the average MWD penetration rate aligns closely with DPM drilling speed, yet remains high levels of random variability. If this randomness could be minimized, it would better reflect changes in the physical properties of the stratigraphic interface, thus providing useful insights for lithological characterization. Moreover, the maximum average penetration rate for MWD along drillhole B is 11.54 m/min, significantly higher than the maximum DPM speed of 2.145 m/min, with a considerable difference also evident in the minimum values. The distribution of MWD average penetration rate is wider, and its CV is markedly higher than that of DPM drilling speed. The digital comparison results of the average MWD penetration rate and DPM penetration rate of drillholes A and B are shown in Table 3. MWD and DPM data along drillhole A present variations of drilling parameters, with the CV reaching 133.3 % and 116.7 %. The similar results along drillhole B also demonstrate substantial variability, with the CV reaching 205.8 % and 275.3 %.

The relationship between drilling data along two drillholes in Table 3 is further explored by calculating confidence interval and significance test. A 95 % confidence interval (CI) estimates the range within which the true data mean is likely to lie, assuming a normal distribution for large samples. Overlapping CIs between groups suggest no significant difference, whereas non-overlapping intervals indicate potential statistical divergence.

$$CI = \bar{x} \pm Z_{\alpha/2}\frac{S}{\sqrt{n}} \tag{6}$$

where $\bar{x}$ is the sample mean, s is the SD, n is the sample size, and $Z_{\alpha/2} = 1.96$ corresponds to the 95 % confidence level.

A paired t-test evaluates whether the mean difference between two related measurements (MWD vs. DPM method along the same drillhole) is statistically significant. The resulting t-statistic is compared to critical values from the t-distribution, and a p-value less than 0.05 rejects the null hypothesis.

$$t = \frac{\bar{d}}{S_d/\sqrt{n}} \tag{7}$$

where $\bar{d}$ is the mean difference, s_d is the SD of the differences, and $Z_{\alpha/2} = 1.96$ corresponds to the 95 % confidence level.

According to Eqs. (6) and (7) and data in Table 3, along drillhole A, the mean difference between MWD and DPM is significant ($p < 0.001$), with MWD yielding higher values (95 % CI: 0.46–0.62) compared to DPM (95 % CI: 0.25–0.31). The large negative percentage difference (−91.1 %) and high variability (SD: −197.1 %) highlight substantial methodological divergence. Along drillhole B, MWD results (95 % CI: 0.39–0.81) were markedly higher than DPM (95 % CI: 0.04–0.10), with an extreme mean difference (−745.1 %, $p < 0.001$). The wider CI for MWD reflects greater data dispersion. Based on the above discussion, these fluctuations may be attributed to variations in geomaterial strength or algorithm-induced random fluctuations. The subsequent subsection will investigate the underlying causes through comparative analysis between the two analytical results and stratigraphic column by site loggings.

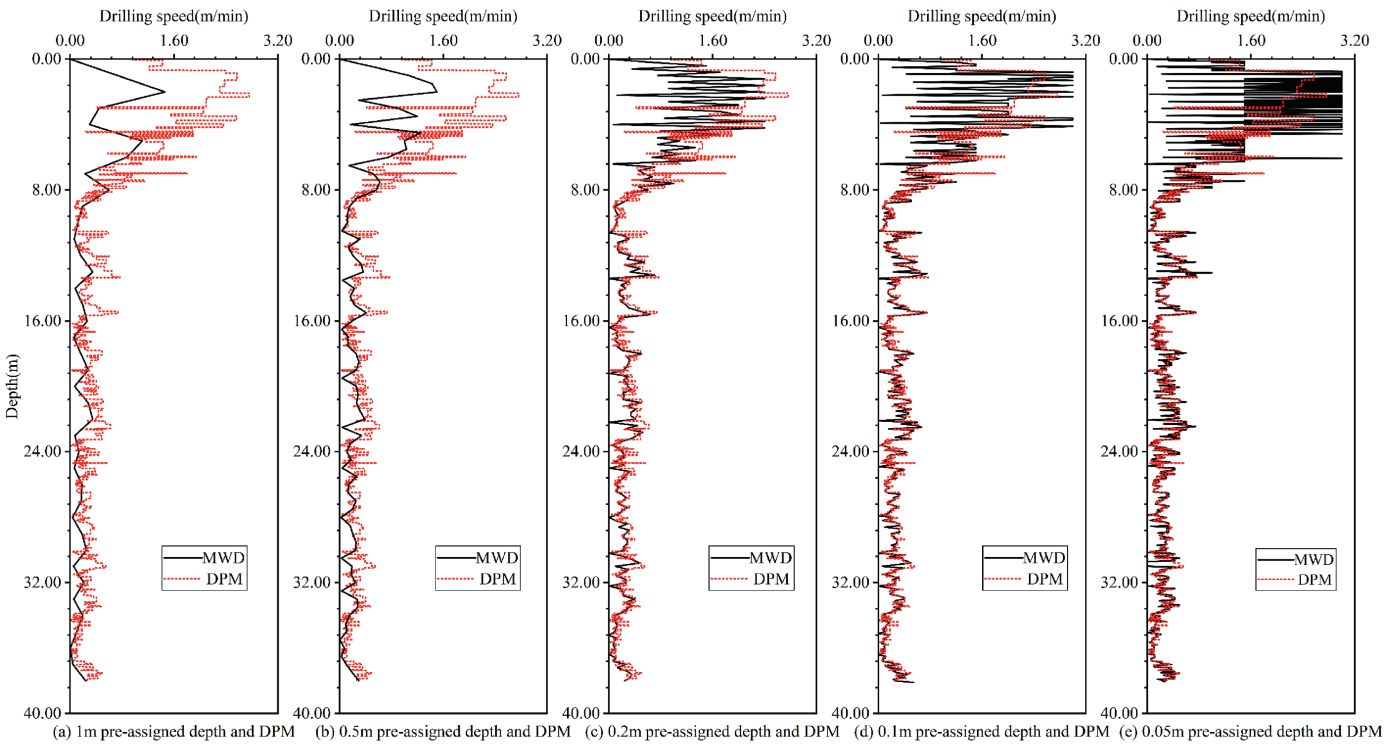

Fig. 9. Drilling depth and drilling time curves for different pre-assigned depths along drillhole A: (a) 1 m pre-assigned depth and DPM, (b) 0.5 m pre-assigned depth and DPM, (c) 0.2 m pre-assigned depth and DPM, (d) 0.1 m pre-assigned depth and DPM, and (e) 0.05 m pre-assigned depth and DPM.

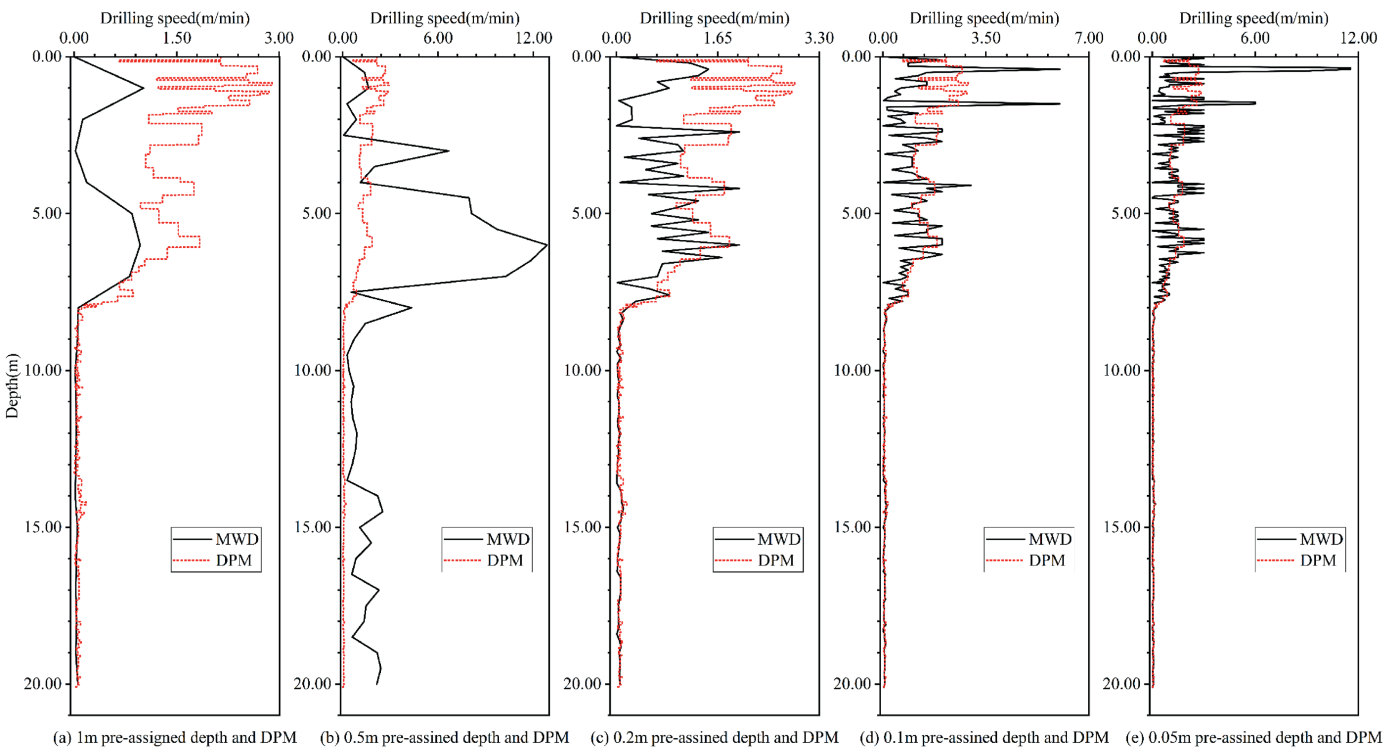

Fig. 10. Drilling depth and drilling time curves of different pre-assigned depths along drillhole B: (a) 1 m pre-assigned depth and DPM, (b) 0.5 m pre-assigned depth and DPM, (c) 0.2 m pre-assigned depth and DPM, (d) 0.1 m pre-assigned depth and DPM, and (e) 0.05 m pre-assigned depth and DPM.

Table 3
The digitized results of MWD average penetration rate and DPM drilling speed along drillhole A and B.

Drillhole	Analysis method	Average penetration rate level (m/min)				Max (m/min)	Mean (m/min)	SD (m/min)	CV (%)
		min	25 %	50 %	75 %				
A	MWD	0.000	0.158	0.300	0.500	3.000	0.537	0.716	133.3
	DPM	0.015	0.104	0.170	0.290	2.760	0.281	0.241	116.7
B	MWD	0.000	0.040	0.070	1.000	11.540	0.600	1.240	205.8
	DPM	0.006	0.024	0.042	0.064	2.145	0.071	0.196	275.3

3.2. Comparison of MWD penetration rate and DPM drilling speed in stratigraphic perspective

This section compares the stratigraphic interface profile, DPM drilling speed and MWD average penetration rate at the pre-assigned depths of 0.05 m and 0.1 m, which can more intuitively analyze the variation trend of drilling speed obtained by different analysis methods or the same method at different preset depths with stratigraphic interface changes. The comparison results of drillhole A are shown in Fig. 11, and the comparison results of drillhole B are shown in Fig. 12.

Fig. 11a is the stratigraphic column chart recorded in the field in drillhole A. Fig. 11b is the curve of DPM drilling speed changing with depth, Fig. 11c is the curve of penetration rate changing with depth when the preset depth is 0.01 m using the MWD method, Fig. 11d is the curve of penetration rate changing with depth when the preset depth is 0.1 m using the MWD method. The dotted lines represent the boundaries of different stratigraphic column. The analysis of drillhole A facilitated a comparison between the average penetration rate of MWD method and DPM drilling speed. The findings indicate that DPM drilling speed responds more sensitively to changes in stratigraphic interface conditions. While the average penetration of MWD method generally correlates with the structural interfaces of the geomaterials, it exhibits varying degrees of random variability across different stratigraphic interface areas.

Notably, the difference in MWD average penetration rate between fill and highly decomposed tuffaceous glutenite stratigraphic interface is substantial, recorded at −326.6 % and −108.8 %, respectively. Although the differences between silty clay and moderately decomposed siltstone stratigraphic interface are relatively smaller, they remain significant at −53.6 % and −62.2 %. In contrast, the variation in gravelly clay and completely decomposed argillaceous siltstone stratigraphic interface is lower, showing −37.3 % and −33.9 %, respectively.

The change levels for highly decomposed argillaceous siltstone, moderately decomposed argillaceous siltstone, and moderately decomposed tuffaceous glutenite stratigraphic interface are quite similar, with values of −9.9 %, −10.6 %, 7.8 %, and 14.9 %, respectively.

Fig. 12a is the stratigraphic column chart recorded in the field in drillhole A. Fig. 12b is the curve of DPM drilling speed changing with depth, Fig. 12c is the curve of penetration rate changing with depth when the preset depth is 0.01 m using the MWD method,

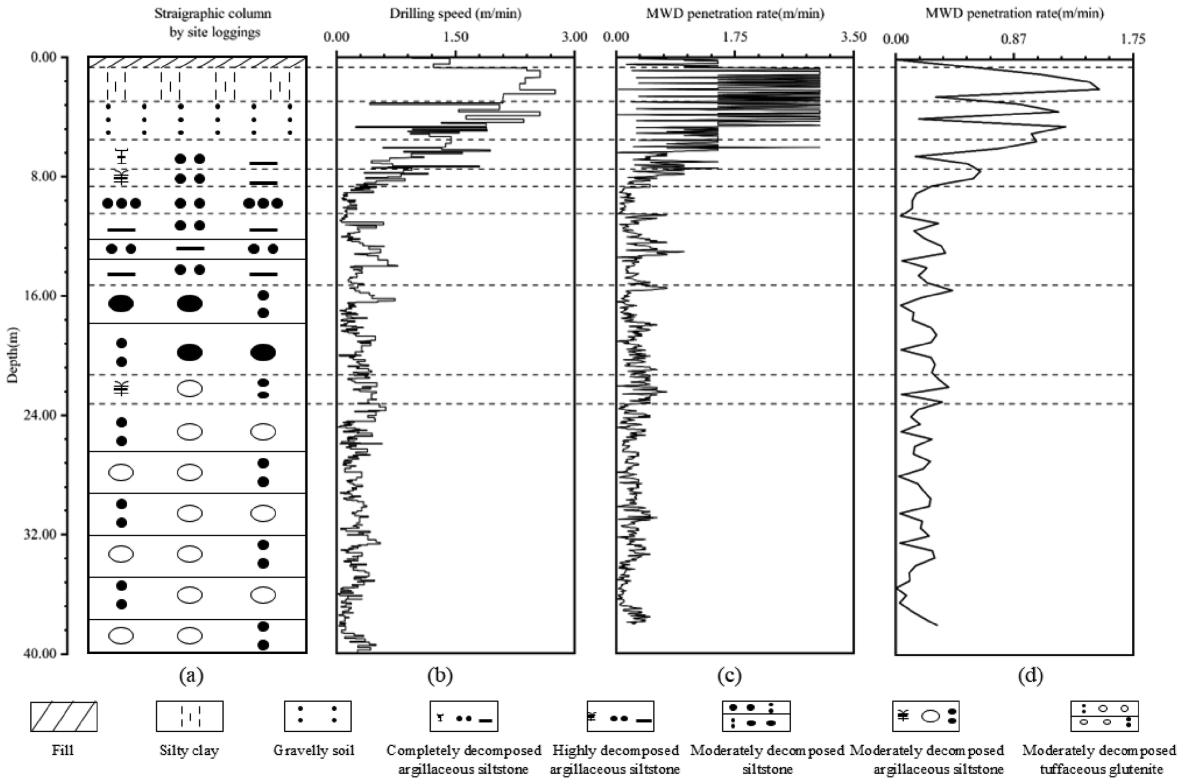

Fig. 11. Relationship between stratigraphic column by site loggings, MWD penetration rate and DPM drilling speed along drill depth along drillhole A: (a) Stratigraphic column by site loggings, (b) DPM drilling speed, (c) 0.01 m pre-assigned depth by MWD, and (d) 0.1 m pre-assigned depth by MWD.

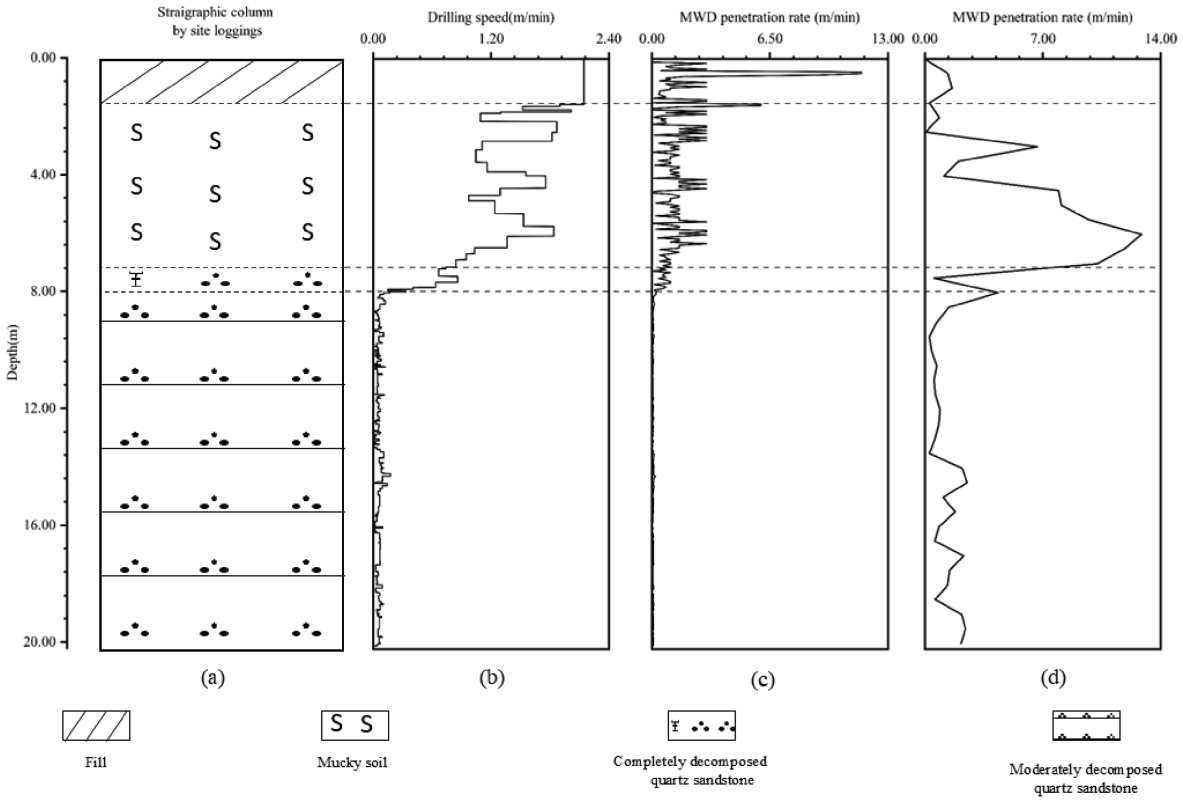

Fig. 12. Relationship between stratigraphic column by site loggings, MWD penetration rate and DPM drilling speed along drill depth along drillhole B: (a) Stratigraphic column by site loggings, (b) DPM drilling speed, (c) 0.01 m pre-assigned depth by MWD, and (d) 0.1 m pre-assigned depth by MWD.

Fig. 12d is the curve of penetration rate changing with depth when the preset depth is 0.1 m using the MWD method. The dotted lines represent the boundaries of different stratigraphic column.

Along drillhole B, the maximum average MWD penetration rate in the Fill area is 11.538 m/min, while the minimum is 0 m/min, resulting in a CV of 126.6 %, indicating an extremely high level of random variation. In contrast, DPM drilling speed in this area remains constant at 2.145 m/min, with a CV of 0 %. In the Mucky Soil area, the maximum average penetration rate for MWD is 3.00 m/min, with a minimum of 0.00 m/min and a CV of 25.7 %. The CV for DPM in this area is 66.7 %, reflecting a difference of 61.5 % between MWD and DPM. For the completely decomposed quartz sandstone area, the maximum average MWD penetration rate again reaches 11.538 m/min, while the minimum is 0 m/min, yielding a CV of 128.6 %, which indicates extremely high random variation. The CV for DPM in this area is 61.0 %, resulting in a difference of 15.0 % compared to MWD. In the moderately decomposed quartz sandstone area, the maximum average MWD penetration rate remains at 11.538 m/min, with a minimum of 0 m/min and a CV of 128.6 %, again demonstrating considerable random variability. The CV for DPM is 51.7 %, while the CV for MWD is 58.6 %, showing a difference of −13.4 %.

The comparative analysis demonstrates that temporal measurements obtained through MWD method (depth-series sampling protocols) constitute a primary source of stochastic deviations in penetration rate quantification. In conventional hydraulic rotary drilling operations, data acquisition by MWD method inherently incorporates ancillary procedures extraneous to pure rock-cutting processes. Such non-productive intervals predominantly induce metrological uncertainties manifested as statistical fluctuations in derived drilling velocity parameters. DPM method effectively mitigates this issue by screening out the net drilling process through time-series-based analytical procedures. It is the reason that DPM method delivers superior accuracy in drilling parameters and stratigraphic interface characterization.

In this case, one XY-1-type hydraulic rotary drilling machine and one polycrystalline diamond compact drill bit were used along two drillholes. The constant drilling speed can also be affected by different drill machines and drill bits. The standardized drill machines and bits can be further studied for the digitalization of drilling parameters as a standard in-situ geotechnical test under different geological environments and drilling conditions.

4. Stratigraphic interface prediction based on drilling parameters

4.1. Feature selection

According to the data analysis results, four types of drilling parameters were collected and analyzed along two drillholes. The drilling speed is related to strength properties of the drilled geomaterials. The downward hydraulic pressure corresponds to the thrust force required to maintain continuous contact between the drill bit and the geomaterial surface while advancing the drill bit to the target depth, whereas the upward hydraulic pressure reflects the retraction force necessary to disengage and elevate the drill string assembly. The rotation data represents the horizontal force to cut the geomaterial surface. These parameters reflect the drilling process and have correlation with the drilled geomaterials.

To determine the features most strongly correlated with stratigraphic interface classification predictions, an enhanced heat map analysis is utilized. This method effectively visualizes the relationships among features and their correlation with the predicted parameters, highlighting their significance. Many features

exhibit minimal impact on the output parameters. Given that a larger dataset increases the computational load on the classifier, it is advisable to eliminate these less influential features. Doing so enhances analysis efficiency, improves model accuracy, and reduces runtime.

Fig. 13 provides several key insights into the interrelationships among various geomaterials physical parameters. The feature correlation heatmap clearly delineates the correlations between five parameters: formation interface, drilling speed, downward pressure, upward pressure, and rotation speed. The square area in the heatmap represents the correlation coefficient between the variables on the horizontal and vertical axes. A larger absolute value of the correlation coefficient indicates a stronger correlation between the two variables. A positive correlation coefficient signifies a positive relationship, while a negative coefficient indicates a negative relationship. A coefficient close to zero suggests little to no correlation. The color intensity of the square represents the strength of the correlation: warmer colors denote positive correlations, and cooler colors indicate negative correlations. Since the labels on both axes are identical, the diagonal of the heatmap shows a correlation coefficient of 1, indicating perfect correlation, and the content on either side of the diagonal is symmetrical.

Notably, along drillhole A, the formation interface exhibits a strong correlation with both drilling speed and upward pressure. It has the highest correlation with drilling speed, with a coefficient of −0.59, suggesting that as the formation interface strength increases, drilling speed decreases. Conversely, it has the lowest correlation with downward pressure, with a coefficient of 0.16. It is because the hydraulic power of the downward pressure during the drilling process is limited to a fixed working gear. Additionally, drilling speed is significantly correlated with upward pressure and rotation speed, with correlation coefficients of −0.55 and 0.39. Similarly, along drillhole B, the stratigraphic interface and drilling speed exhibit a strong correlation, with a correlation coefficient of −0.7. In contrast, the correlation between rotation speed and the formation interface remains the weakest, with a coefficient of 0.18. Upward and downward pressures show some correlation, with coefficients of 0.32 and −0.26, respectively. Along both drillholes A and B, drilling speed has the strongest correlation with the stratigraphic interface, and they are negatively correlated; as the formation interface strength increases, the drilling speed decreases. The weakest correlation is with rotation speed. The differing correlation coefficients between the two drillholes are primarily due to variations in stratigraphic interface conditions and sample sizes.

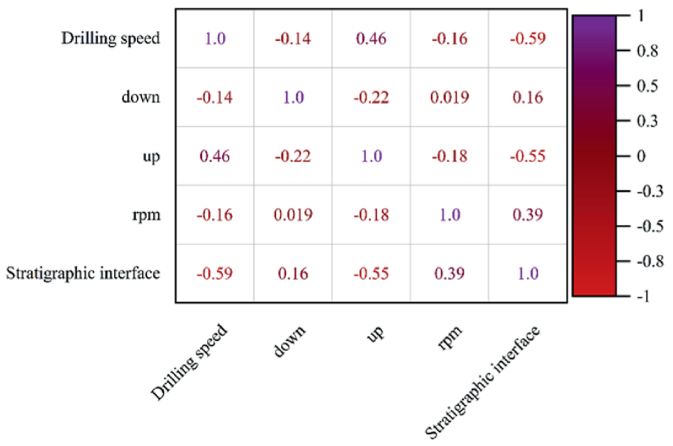

(a) Parameter thermal correlation diagram along drillhole A

(b) Parameter thermal correlation diagram along drillhole B

Fig. 13. Parameter thermal correlation diagram: (a) Drilling parameters along drillhole A, and (b) Drilling parameters along drillhole B.

4.2. Prediction of stratigraphic interface profiles based on drilling parameters

Stratigraphic interface profile prediction is vital in geological research, significantly impacting stratigraphic division and comparison (Zhang et al., 2018; Saadati et al., 2024). Drilling parameters like drilling speed, rotation speed, upward pressure, and downward pressure provide valuable indicators for stratigraphic interface stratification, as they contain extensive stratigraphic information. However, the effectiveness of these parameters in differentiating between various stratigraphic interfaces and substrata can vary.

This paper utilizes the SVM (support vector machine) algorithm, a machine learning approach to predict stratigraphic interface profiles. Although core sampling and logging profiles are reliable for acquiring lithological information, their high costs often restrict sampling to reservoir sections or specific stratigraphic areas of interest. As a result, stratigraphic interface classification often faces challenges due to small sample sizes, especially when compared to prediction tasks involving parameters like drilling speed (Barbosa et al., 2019). The SVM algorithm is particularly advantageous due to its strong generalization capabilities. It operates on the principle of structural risk minimization and is rooted in statistical learning theory tailored for finite sample scenarios. The SVM algorithm effectively addresses the small sample problem associated with geomaterials strength prediction, making it a valuable tool for stratigraphic interface profile prediction (Bressan et al., 2020; Maepa et al., 2021).

The prediction parameters selected are presented in Table 4, while the corresponding prediction results are displayed in Table 5. Analysis of the stratigraphic interface classification results for drillholes A and B indicates that the model demonstrates strong predictive capability for data analyzed by DPM method, while it exhibits relatively weaker performance for data analyzed by MWD method. The accuracy of the training and test sets derived from MWD method is significantly lower than that obtained from DPM method. Furthermore, there is a noticeable gap in

Table 4
SVM prediction parameters.

Item	Value
Penalty factor	1.00
Kernel function coefficients	28.594
Kernel Function	RBF kernel

Table 5
SVM prediction results based on data obtained by MWD and DPM analyzing methods.

Drillholes	Training set accuracy (%)		Test set accuracy (%)	
	DPM	MWD	DPM	MWD
A	78.54	58.20	77.81	57.24
B	99.31	60.12	99.26	61.25

prediction accuracy between the parameters based on drillhole A and those based on drillhole B. This discrepancy arises because the SVM algorithm is primarily designed for learning from small sample sizes and may struggle with larger datasets.

Overfitting may arise in SVM models when complex kernel functions excessively capture noise or non-generalizable patterns in the limited drilling data, leading to poor generalization on unseen formations. To mitigate this issue, the following steps are used:

(1) Regularization (tuning parameter C) can balance margin width and classification errors;
(2) Kernel selection (e.g. linear or low-complexity kernels) reduces model flexibility;
(3) Cross-validation optimizes hyperparameters; and
(4) Feature prioritizes geologically meaningful drilling parameters (e.g. drilling speed and downward pressure) over redundant metrics.

Additionally, further studies on enlarging the training dataset with diverse lithology scenarios can enhance robustness against overfitting.

5. Conclusions

This study investigated the disparities in drilling parameters between MWD and DPM across two distinct drillholes and evaluated their impact on geomaterial property prediction. The results revealed significant random variability in MWD-derived penetration rates, whereas the DPM method exhibited minimal stochastic fluctuations due to its real-time data segmentation into homogeneous sub-zones. These sub-zones demonstrated drilling speeds that closely aligned with actual stratigraphic distributions. Along drillhole A, the difference between the average MWD penetration rate and DPM drilling speed was 91.7 %, with a SD of 197.1 %. Along drillhole B, the difference reached 745.1 %, with a SD of 532.7 %.

(1) Parametric analysis demonstrated that operational parameters (downward pressure, upward pressure, rotation speed) within typical ranges exerted negligible influence on drilling speed in straight drillhole segments. Stratigraphic strength resistance was identified as the primary factor governing drilling speed variations, with significant negative correlations observed between interface strength and velocity. It means that an increase of stratigraphic strength corresponds to a decrease of drilling speed. The disparity in correlation coefficients between drillholes primarily resulted from differences in formation conditions and parameter sample sizes.
(2) The SVM algorithm was implemented to benchmark lithological classification performance between MWD depth-series data and DPM real-time data. This comparative analysis revealed fundamental limitations in MWD's stratigraphic interface prediction accuracy relative to DPM. It confirms that MWD methodologies cannot ensure drilling information reliability while establishing a causal relationship between measurement inconsistencies and compromised stratigraphic profile predictions.
(3) Comparative analysis demonstrates that DPM delivers superior accuracy in drilling parameters and stratigraphic interface characterization, particularly through its real-time processing capacity in geologically complex environments. The accuracy-stability balance substantiates DPM's extensive applicability across geological and geotechnical engineering. Future studies should prioritize hybrid algorithmic architectures to achieve synergistic improvements in analytical precision and operational efficiency. On one hand, more real-time drilling parameters under different geological environments and drilling conditions can be collected to further investigate the strength and structural characteristics of drilled geomaterials. On the other hand, by integrating drilling-process monitoring with drillhole imaging techniques, machine learning or deep learning approaches can be employed to perform multi-source data fusion analysis for evaluating the engineering rock mass quality. This comprehensive methodology aims to improve the accuracy of stratigraphic profiles and guide subsequent engineering decisions.

CRediT authorship contribution statement

Ping-Feng Li: Methodology, Writing – original draft, Writing – review & editing, Conceptualization, Project administration, Formal analysis, Funding acquisition, Data curation. **Xue-Fan Wang:** Funding acquisition, Methodology, Project administration, Investigation, Writing – original draft, Data curation, Writing – review & editing, Formal analysis, Supervision, Conceptualization. **Zhou Yang:** Data curation, Investigation, Methodology, Formal analysis, Writing – review & editing, Visualization. **Zhong-Jian Zhang:** Formal analysis, Project administration, Writing – review & editing, Investigation, Conceptualization. **Fei Yang:** Investigation, Validation, Data curation. **Hong-Pei Tang:** Data curation, Validation. **Bing-Bing Zhang:** Data curation, Validation.

Declaration of competing interest

The authors declare that they have no known competing financial interests or personal relationships that could have appeared to influence the work reported in this paper.

Acknowledgments

The paper was partially supported by Deep Earth Probe and Mineral Resources Exploration - National Science and Technology Major Project (Grant No. 2024ZD1003406), National Natural Science Foundation of China (Grant No. 42302312), and the Fundamental Research Funds for the Central Universities (Grant No. 2-9-2022-013).

References

Alipour, M., 2024. Petroleum systems of the Iranian Zagros fold and thrust belt. Res. Earth Sci. 2, 100027.
Bahrami, S., Ehteshami-Moinabadi, M., Tuyserkani, M.S., 2024. Quantitative evaluation of morphometric parameters of drainage system in the forelimb and backlimb of the Asmari Anticline, Zagros, Iran. J. Struct. Geol. 184, 105151.
Barbosa, L.F.F., Nascimento, A., Mathias, M.H., De-Carvalho Jr, J.A., 2019. Machine learning methods applied to drilling rate of penetration prediction and optimization-A review. J. Pet. Sci. Eng. 183, 106332.
Bressan, T.S., De-Souza, M.K., Girelli, T.J., Junior, F.C., 2020. Evaluation of machine

learning methods for lithology classification using geophysical data. Comput. Geosci. 139, 104475.
Chen, C., Ji, G., Wang, H., Huang, H., Baud, P., Wu, Q., 2022. Geology-engineering integration to improve drilling speed and safety in ultra-deep clastic reservoirs of the Qiulitage structural belt. Adv. Geo-Energy Res. 6 (4), 347–356.
Chen, J., Yue, Z.Q., 2015. Ground characterization using breaking-action-based zoning analysis of rotary-percussive instrumented drilling. Int. J. Rock Mech. Min. Sci. 75, 33–43.
Deng, N., Qiao, L., Li, Q., Zhang, Q., Hao, J., 2024. True-scale mapping of rock discontinuities from single images without calibration. Tunn. Undergr. Space Technol. 152, 105859.
Fortunati, F., Pelligrino, G., 1998. The Use of Electronics in the Management of Site Investigation and Soil Improvement Works: Principles and Applications. Geotechnical Site, pp. 359–364.
Garassino, A., Schinelli, M., 1998. Detection of cavities by monitored borehole dirlling (TMD). Geotechnical Site 365–370.
Gui, M.W., 2008. The basics of noise detection and filtering for borehole drilling data. Open Civ. Eng. J. 2 (1), 113–120.
Gui, M.W., Soga, K., Bolton, M., Hamelin, J., 2002. Instrumented borehole drilling for subsurface investigation. J. Geotech. Eng. 128 (4), 283–291.
Handhal, A.M., Ettensohn, F.R., Al-Abadi, A.M., Ismail, M.J., 2022. Spatial assessment of gross vertical reservoir heterogeneity using geostatistics and GIS-based machine-learning classifiers: a case study from the Zubair formation, Rumaila oil field, Southern Iraq. J. Pet. Sci. Eng. 208, 109482.
He, P., Chen, Y., Jiang, F., Wang, G., Jiang, Y., 2024. An approach to rapidly evaluating rock mass quality in underground engineering based on multi-source heterogeneous data. Rock Mech. Rock Eng. 58, 1295–1325.
Jalili, Y., Yassaghi, A., Khatib, M.M., Golalzadeh, A., 2020. Effect of transverse faults on fracture characteristics and borehole instability in the Asmari reservoir of Zagros folded belt zone, Iran. J. Pet. Sci. Eng. 188, 106820.
Jamshidi, E., Kianoush, P., Hosseini, N., Adib, A., 2024. Scaling-up dynamic elastic logs to pseudo-static elastic moduli of rocks using a wellbore stability analysis approach in the Marun oilfield, SW Iran. Sci. Rep. 14 (1), 19094.
Jimeno, C.L., Jimeno, E.L., Carcedo, F.J.A., De-Ramiro, Y.V., 1995. Drilling Änd Blasting of Rocks, vol. 41. USA CRS Press, 35947.
Kianoush, P., Mohammadi, G., Hosseini, S.A., Keshavarz-Faraj, K.N., Afza, P., 2022. Application of pressure-volume (PV) fractal models in modeling formation pressure and drilling fluid determination in an oilfield of SW Iran. J. Pet. Sci. Technol. 12 (1), 2–20.
Li, S., Liu, B., Xu, X., Nie, L., Liu, Z., Song, J., Sun, H., Chen, L., Fan, K., 2017. An overview of ahead geological prospecting in tunneling. Tunn. Undergr. Space Technol. 63, 69–94.
Li, Z., Itakura, K.I., Ma, Y., 2014. Survey of measurement-while-drilling technology for small-diameter drilling machines. Electron. J. Geotech. Eng. 19 (Z2), 10267–10282.
Liu, L., Li, S., Zheng, M., Wang, D., Chen, M., Zhou, J., Yan, T., Shi, Z., 2024a. Inverting the rock mass P-wave velocity field ahead of deep buried tunnel face while borehole drilling. Int. J. Min. Sci. Technol. 34 (5), 681–697.
Liu, L., Li, S., Zheng, M., Wang, Y., Shen, J., Shi, Z., Xia, C., Zhou, J., 2024b. Identification of rock discontinuities by coda wave analysis while borehole drilling in deep buried tunnels. Tunn. Undergr. Space Technol. 153, 105969.
Long, S., Yue, Z., Yue, W.V., Hu, H., Feng, Y., Yan, Y., Xie, X., 2024. Identification of rock layer interface characteristics using drilling parameters. Rock Mech. Rock Eng. 58, 1071–1098.
Maepa, F., Smith, R.S., Tessema, A., 2021. Support vector machine and artificial neural network modelling of orogenic gold prospectivity mapping in the Swayze greenstone belt, Ontario, Canada. Ore Geol. Rev. 130, 103968.
Mohammadrezaei, H., Alavi, S.A., Cardozo, N., Ghassemi, M.R., 2020. Deciphering the relationship between basement faulting and two-phase folding in the Hendijan anticline, northwest Persian Gulf, Iran. Mar. Petrol. Geol. 122, 104626.
Mostofi, M., Rasouli, V., Mawuli, E., 2011. An estimation of rock strength using a drilling performance model: a case study in blacktip field, Australia. Rock Mech. Rock Eng. 44, 305–316.
Peck, J., Vynne, J., 1993. Current Status and Future Trends of Monitoring Technology for Drills. Australasian Inst of Mining & Metallurgy, Parkville (AUST), pp. 311–325.
Pfister, P., 1985. Recording drilling parameters in ground engineering. Ground Eng. 18 (3), 16–21.
Pireh, A., Alavi, S., Ghassemi, M., Shaban, A., 2015. Analysis of natural fractures and effect of deformation intensity on fracture density in Garau formation for shale gas development within two anticlines of Zagros fold and thrust belt, Iran. J. Pet. Sci. Eng. 125, 162–180.
Pirhadi, A., Kianoush, P., Varkouhi, S., Shirinabadi, R., Shirazy, A., Shirazi, A., Ebrahimabadi, A., 2025. Thermo-poroelastic analysis of drilling fluid pressure and temperature on wellbore stresses in the Mansouri oilfield, SW Iran. Res. Earth Sci. 3, 100061.
Rai, P., Schunesson, H., Lindqvist, P.-A., Kumar, U., 2015. An overview on measurement-while-drilling technique and its scope in excavation industry. J. Inst. Eng.: Series D 96, 57–66.
Saadati, G., Javankhoshdel, S., Mohebbi Najm Abad, J., Mett, M., Kontrus, H., Schneider-Muntau, B., 2024. AI-Powered geotechnics: enhancing rock mass classification for safer engineering practices. Rock Mech. Rock Eng. 1–31.
Schunnesson, H., 1998. Rock characterisation using percussive drilling. Int. J. Rock Mech. Min. Sci. 35 (6), 711–725.
Shechtman, O., 2013. The coefficient of variation as an index of measurement reliability. Methods Clin. Epidemiol. 39–49.
Song, Z., Jing, P., Nie, L., Mei, Z., Jia, S., Li, Z., 2025. Comprehensive identification and assessment of clastic rock and water-bearing breccia for water and mud inrush in tunnel: a case study. Tunn. Undergr. Space Technol. 155, 106156.
Tian, S., Hou, S., Ding, W., Liang, S., Liu, D., Xie, K., Lu, X., Yang, W., 2024. Rock fracture identification with measurement while drilling data in down-the-hole drills. Bull. Eng. Geol. Environ. 83 (2), 65.
van-Eldert, J., Schunnesson, H., Johansson, D., Saiang, D., 2020. Application of measurement while drilling technology to predict rock mass quality and rock support for tunnelling. Rock Mech. Rock Eng. 53 (3), 1349–1358.
Wang, M., Zhou, J., Chen, J., Jiang, N., Zhang, P., Li, H., 2023a. Automatic identification of rock discontinuity and stability analysis of tunnel rock blocks using terrestrial laser scanning. J. Rock Mech. Geotech. Eng. 15 (7), 1810–1825.
Wang, Q., Gao, H., Yu, H., Jiang, B., Liu, B., 2019. Method for measuring rock mass characteristics and evaluating the grouting-reinforced effect based on digital drilling. Rock Mech. Rock Eng. 52 (3), 841–851.
Wang, X., Peng, P., Shan, Z., Yue, Z., 2023b. In situ strength profiles along two adjacent vertical drillholes from digitalization of hydraulic rotary drilling. J. Rock Mech. Geotech. Eng. 15 (1), 146–168.
Wang, X., Wang, C., Yue, W., Zhang, Z., Yue, Z., 2024. In situ digital testing method for quality assessment of soft soil improvement with polyurethane. J. Rock Mech. Geotech. Eng. 16 (5), 1732–1748.
Wang, X.F., Peng, P., Yue, W.V., Shan, Z.G., Yue, Z.Q., 2023c. A case study of drilling process monitoring for geomaterial strength assessment along hydraulic rotary drillhole. Bull. Eng. Geol. Environ. 82 (8), 295.
Wang, X.F., Zhang, M.S., Yue, Z.Q., 2021. In-situ digital profiling of soil to rock strength from drilling process monitoring of 200 m deep drillhole in loess ground. Int. J. Rock Mech. Min. Sci. 142, 104739.
Wang, X.F., Zhang, Z.J., Yue, W.V., Yue, Z.Q., 2023d. Digitalization of hydraulic rotary drilling process for continuously mechanical profiling of siliciclastic sedimentary rocks. Sci. Rep. 13 (1), 3701.
Wu, S.Y., Yue, W.V., Qiu, M., Yue, Z.Q., 2024. Profiling of weathered argillaceous limestone rock with MWD data from advanced drilling for tunnelling along Wu-Kai expressway in Chongqing, China. Tunn. Undergr. Space Technol. 147, 105719.
Wu, S.Y., Yue, W.V., Yue, Z.Q., 2023. On drilling speed of London Clay from MWD data with time-series algorithm for ground characterisation. Geotechnique 75 (2), 166–179.
Xie, J., Huang, J., Zhang, F., He, J., Kang, K., Sun, Y., 2024. Enhancing the resolution of sparse rock property measurements using machine learning and random field theory. J. Rock Mech. Geotech. Eng. 16 (10), 3924–3936.
Xu, Z., Yu, T., Lin, P., Wang, W., Shao, R., 2022. Integrated geochemical, mineralogical, and microstructural identification of faults in tunnels and its application to TBM jamming analysis. Tunn. Undergr. Space Technol. 128, 104650.
Yue, W.V., Wu, S., He, M., Qiao, Y., Yue, Z.Q., 2024. Digital monitoring of rotary-percussive drilling with down-the-hole hammer for profiling weathered granitic ground. J. Rock Mech. Geotech. Eng. 16 (5), 1615–1636.
Yue, Z., Lee, C.F., Law, K.T., Tham, L.G., Sugawara, J., 2002. Use of HKU drilling process monitor in slope stabilization. Chin. J. Rock Mech. Eng. 21 (11), 1685–1690 (in Chinese).
Yue, Z.Q., 2014. Drilling process monitoring for refining and upgrading rock mass quality classification methods. Chin. J. Rock Mech. Eng. 33 (10), 1977–1996 (in Chinese).
Yue, Z.Q., Lee, C.F., Law, K.T., Tham, L.G., 2004. Automatic monitoring of rotary-percussive drilling for ground characterization - illustrated by a case example in Hong Kong. Int. J. Rock Mech. Min. Sci. 41 (4), 573–612.
Zhang, G., Wang, Z., Chen, Y., 2018. Deep learning for seismic lithology prediction. Geophys. J. Int. 215 (2), 1368–1387.
Zhao, R., Shi, S., Yao, R., Yang, S., 2024. Application of relationship model for the measurement while drilling data to predict rock uniaxial compressive strength for tunneling. Rock Mech. Rock Eng. 57 (9), 1–17.

Dr. Xue-Fan Wang is Associate Professor at China University of Geosciences (Beijing), China. He obtained Bachelor and Master degrees in Geological Engineering from Nanjing University, China. He obtained PhD in Geotechnical Engineering at The University of Hong Kong (HKU), China. He was the recipient of Young Elite Scientists Sponsorship Program by CAST. His research has been funded by multiple national grants, and the outcomes have been applied to major infrastructure projects. His main expertise includes intelligent monitoring techniques for various applications in geological engineering and civil engineering. His research interests cover drilling process monitoring (DPM), measurement while drilling (MWD), distributed fiber optical sensing, digitalization, and artificial intelligence.